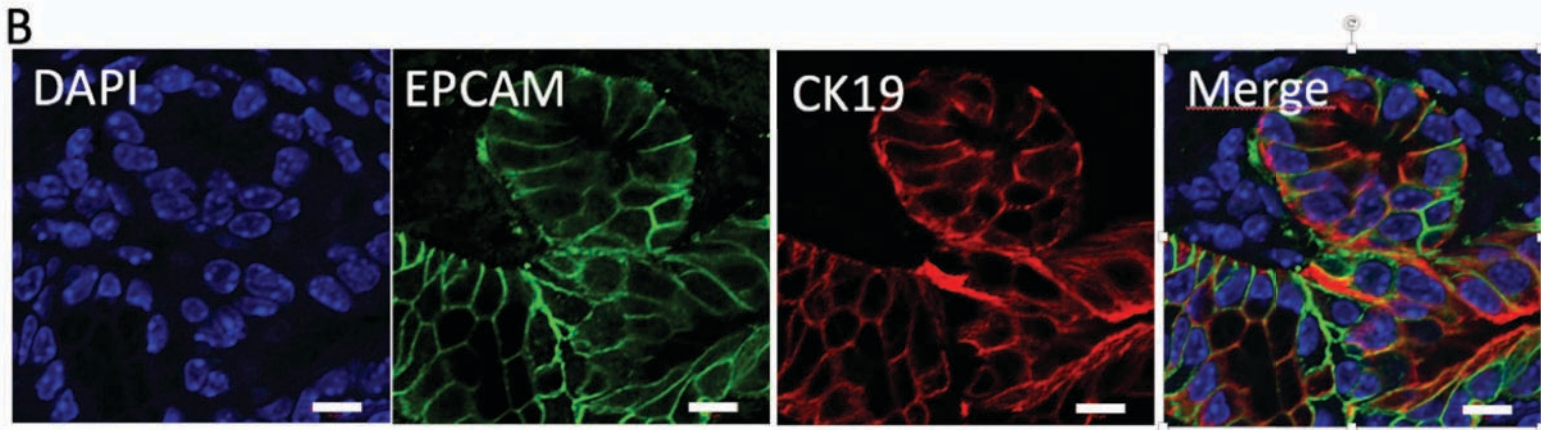
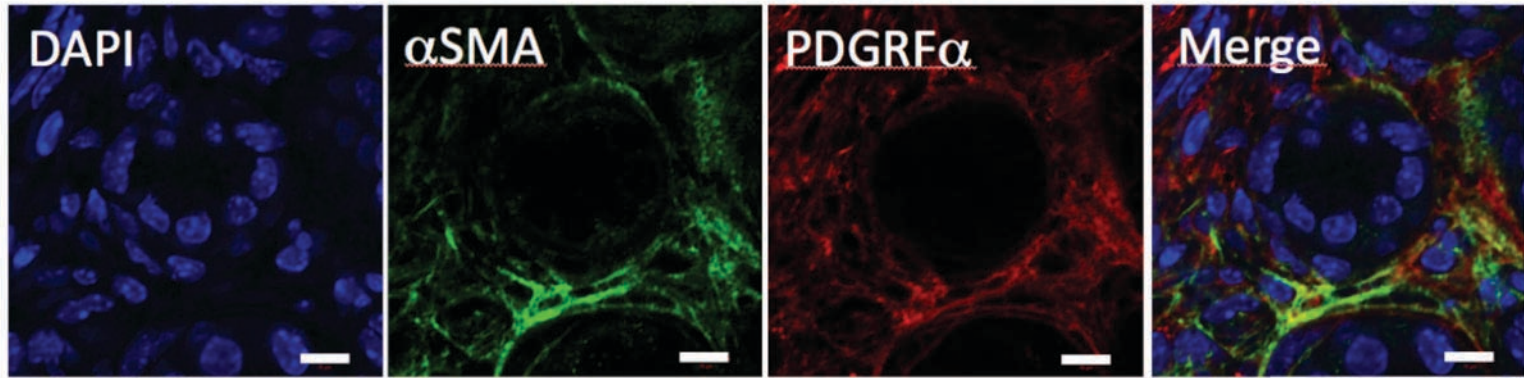


**Supplementary Figure 1.** Representative immunohistochemical staining for  $\beta$ ig-h3 in the pancreas in 8 PDA patients. Scale bar, 100  $\mu$ m. Quantification of the areas of  $\beta$ ig-h3 staining in KC mice at different ages, in KIC and KPC mice as well as in a cohort of 12 patients with PDAC. Two representative pictures of patient 12 showing no expression in adjacent non tumoral tissue.



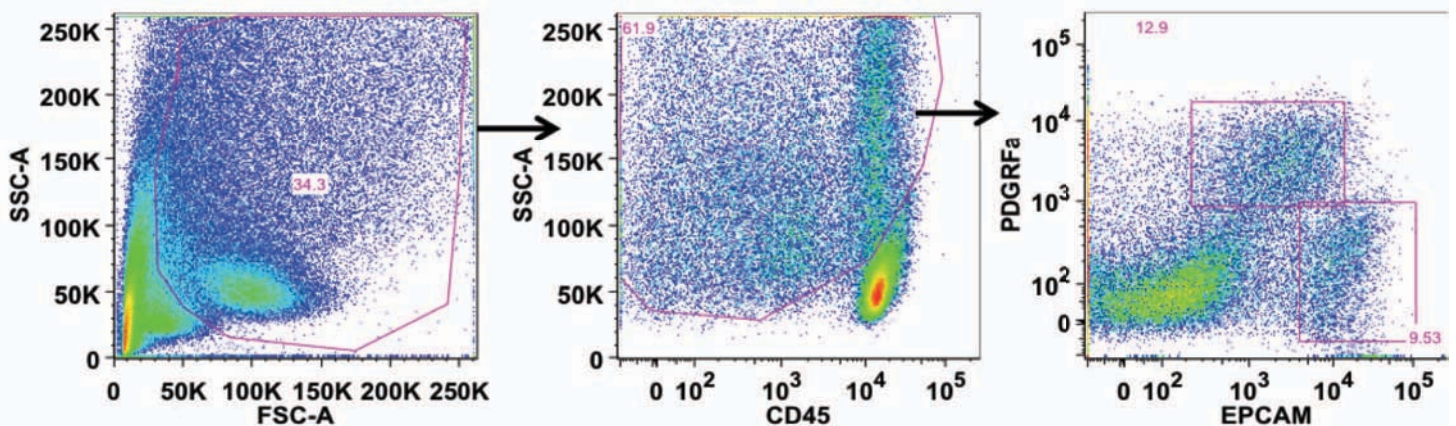


C

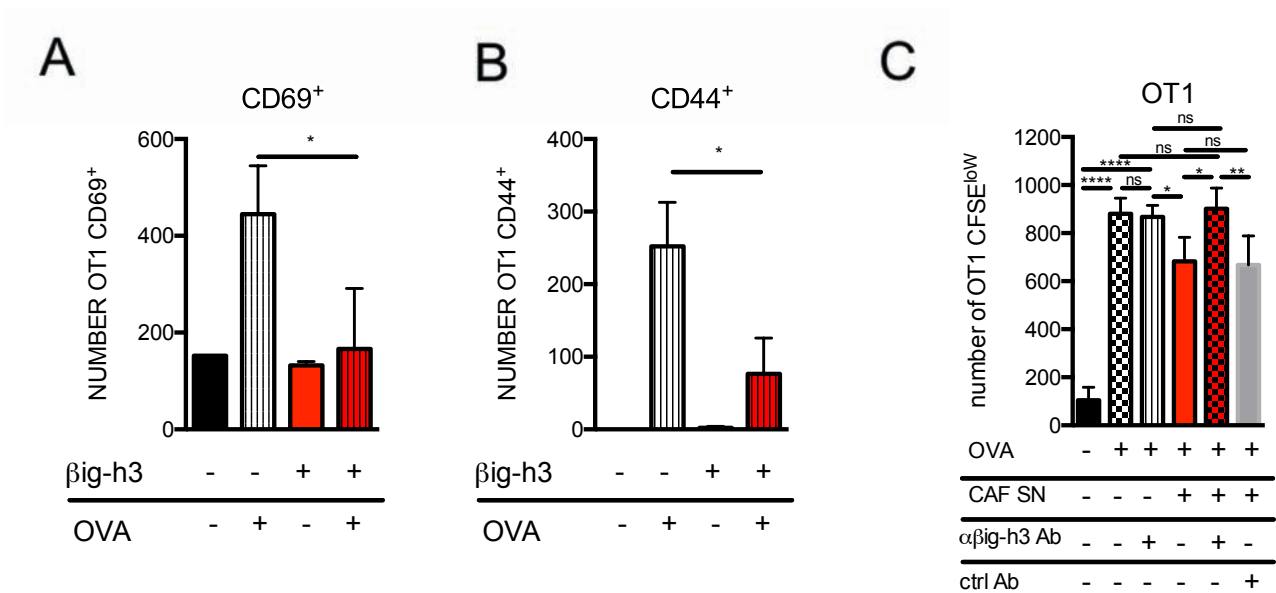
### Ductal and CAF cell isolation



### Gating strategy



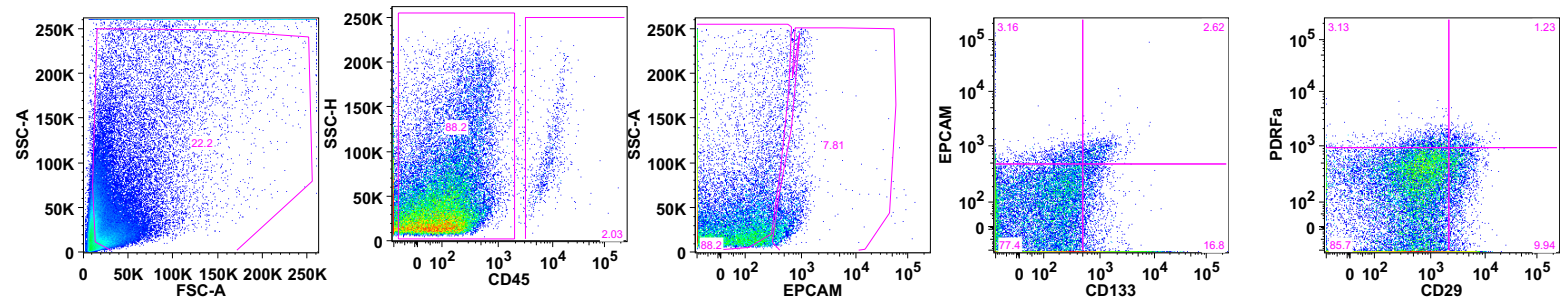
**Supplementary Figure 2.** Representative immunofluorescence labeling in the pancreas in KC mice for  $\alpha$ SMA and EPCAM (green), PDGFR $\alpha$  and CK19 (red) and DAPI (blue) (A, B). Scale bar, 10  $\mu$ m. (C) The gating strategy used to isolate ductal cells and CAFs.



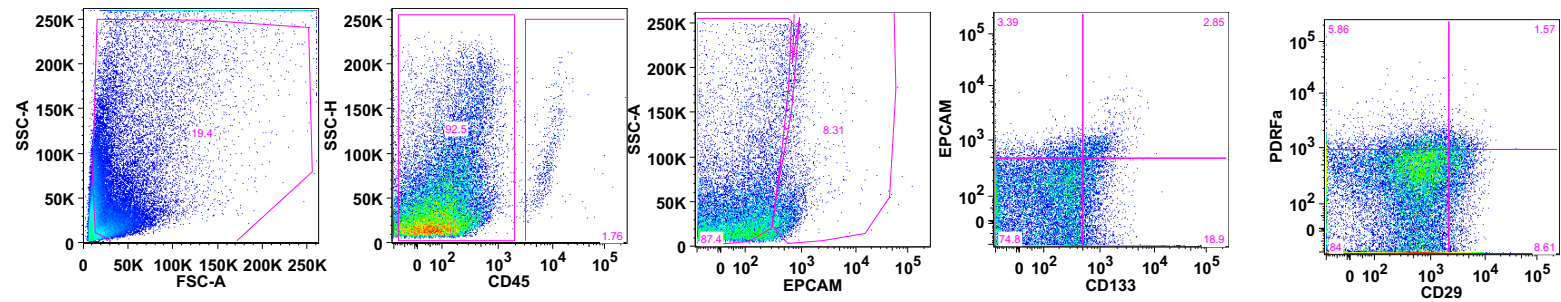
**Supplementary Figure 3** CFSE-labeled OT1 splenocytes were cultured in the presence or absence of rβig-h3 (5 μg/ml) and activated using OVA peptide at a concentration of 1 μg/ml for 72 h. The graphs demonstrate the number of CFSE<sup>low</sup> OT1 T cells that expressed CD69 (A) or CD44 (B). CFSE-labeled OT1 splenocytes were cultured in the presence/absence of CAF supernatant (C) in the presence of anti-βig-h3 antibodies or ctrl antibodies and activated using OVA peptide (1 μg/ml) for 72 h. The graphs demonstrate the number of CFSE<sup>low</sup> OT1 cells. One way Anova and Tukey's multiple comparisons tests were performed. \*\*\*\*  $P < 0.0001$ , \* $P < 0.05$ , \*\* $P < 0.01$ .

**Phenotype  
KC cell line**

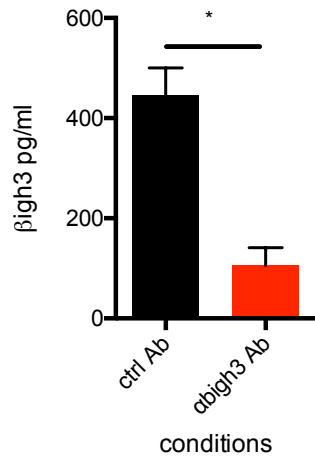
A



**Phenotype  
KIC cell line**

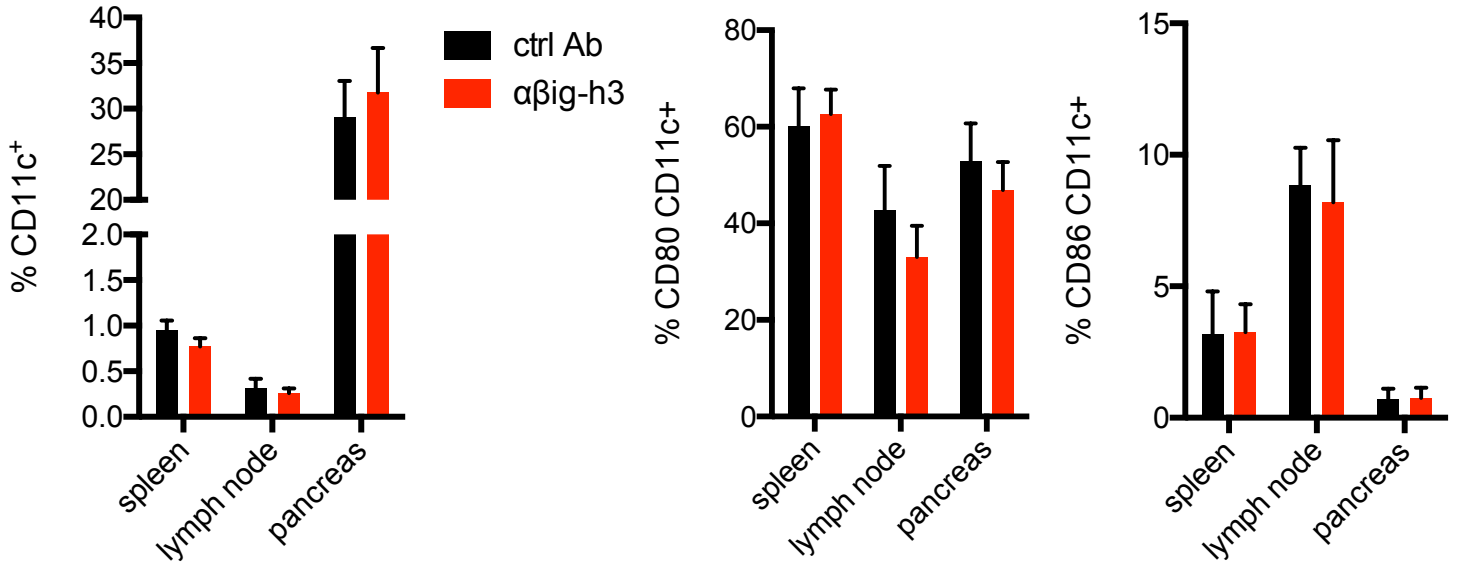


B

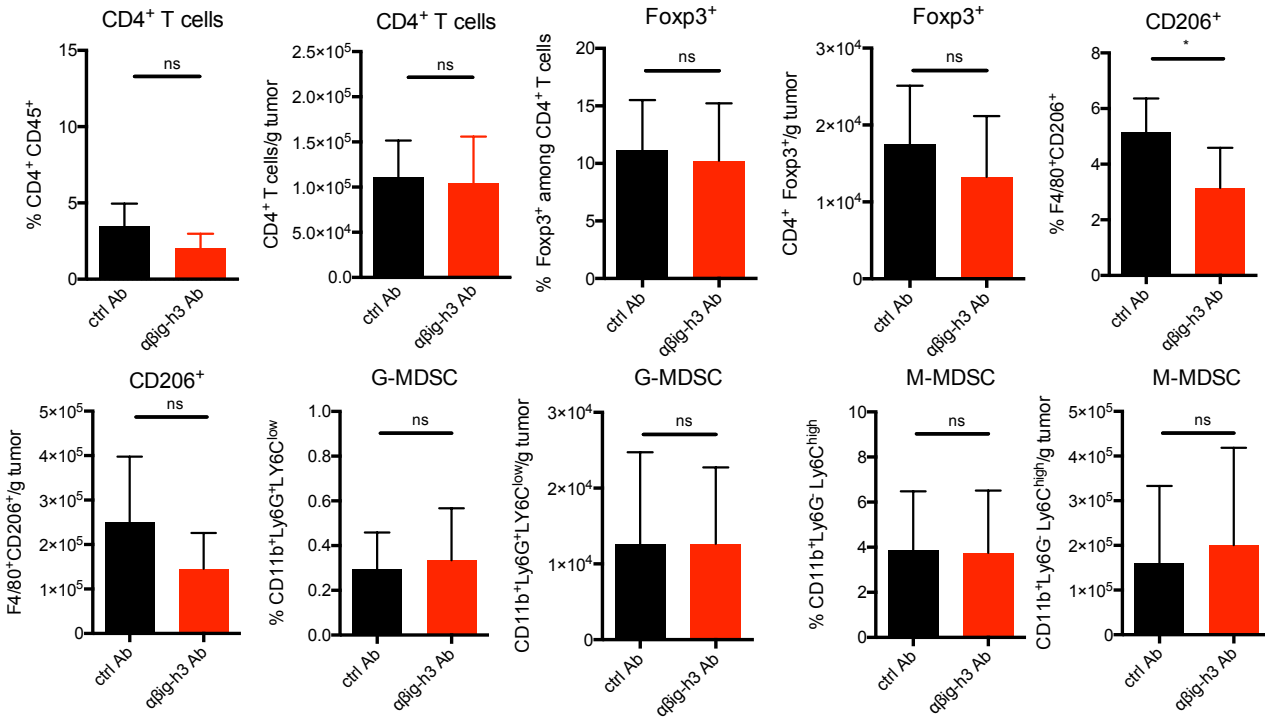


**Supplementary Figure 4.** (A) Representative immunofluorescence labeling of KC and KIC cell lines. (B) ELISA was used to quantify the level of  $\beta$ ig-h3 secreted by KC cells incubated in the presence of anti- $\beta$ ig-h3 or ctrl antibodies. \* $P < 0.05$

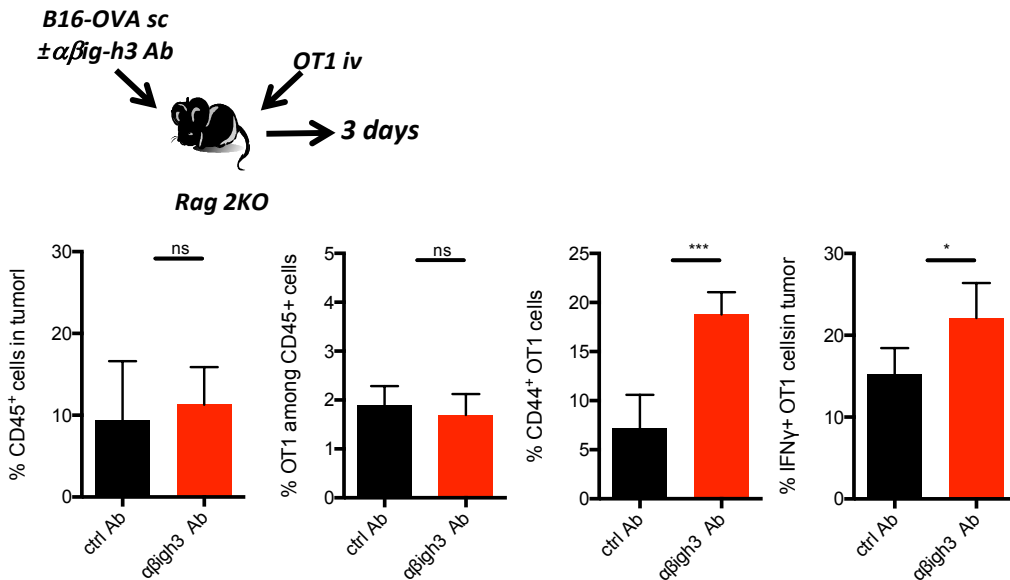
A



B



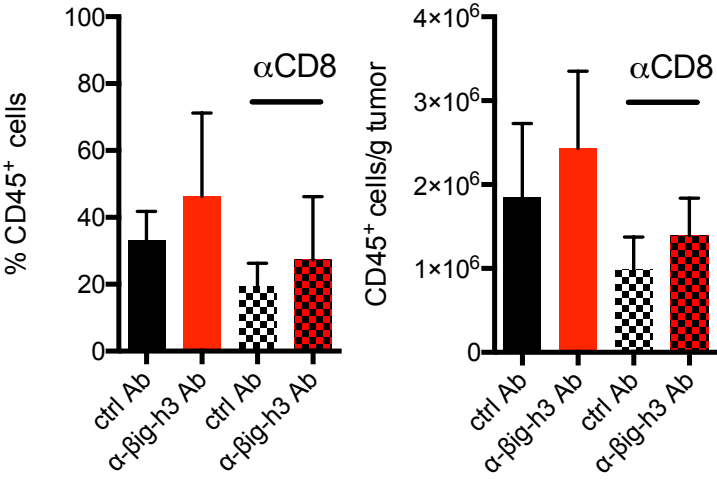
C



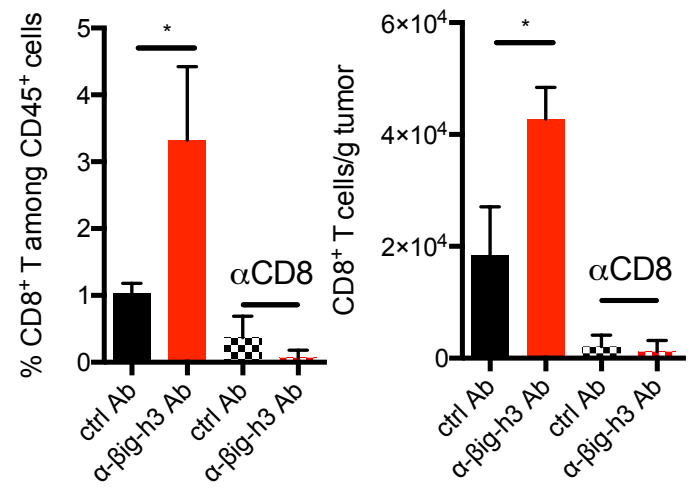
**Supplementary Figure 5.** FACS analysis of the following immune cell populations: (A) % CD11c, % CD80 among CD11c<sup>+</sup> cells, % CD86<sup>+</sup> among CD11c<sup>+</sup> cells; (B) % and numbers/g tumor CD4<sup>+</sup> T cells, CD4<sup>+</sup> Foxp3<sup>+</sup> T cells, F4/80<sup>+</sup>CD206<sup>+</sup> macrophages Gr-MDSC, Mo-MDSC in C57Bl6 mice that were subcutaneously injected with KC cells that were treated with ctrl or anti-βig-h3 antibodies. (C) B16 OVA cells (+ anti-βig-h3 Ab or ctrl Ab) were s.c. injected in Rag2<sup>KO</sup> mice i.v. transferred with OT1 cells. Graphs represent % CD45 cells within the tumor, % OT1 among CD45<sup>+</sup> cells, % OT1 CD44<sup>high</sup> and % OT1 IFNγ<sup>+</sup>, \**P* < 0.05. \*\*\**P* < 0.001.



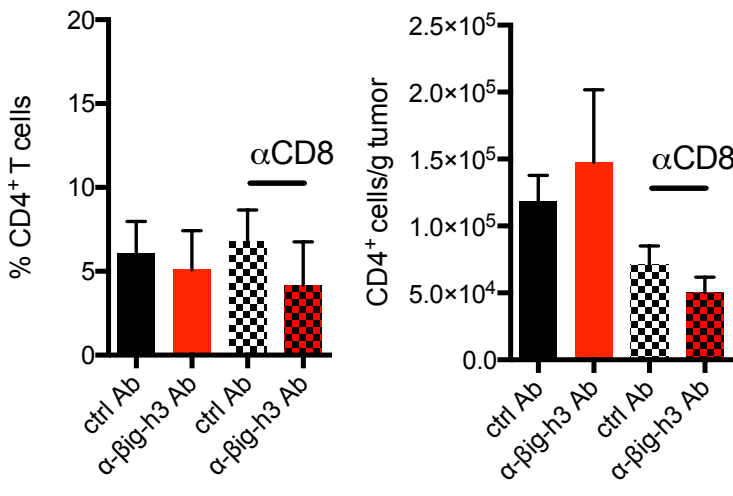
**A**



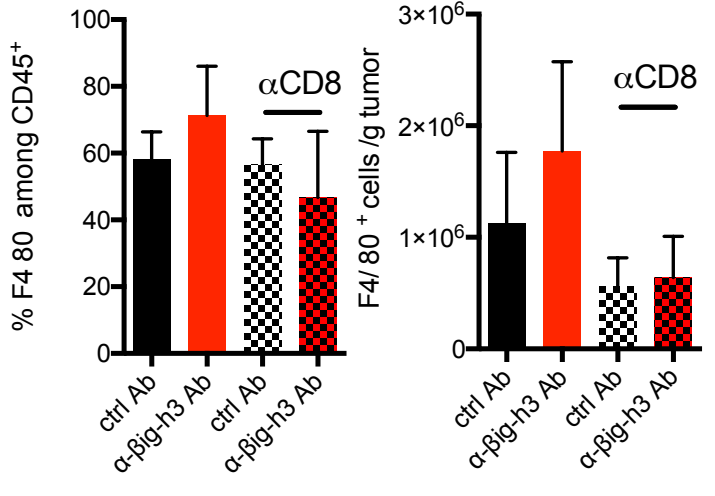
**B**



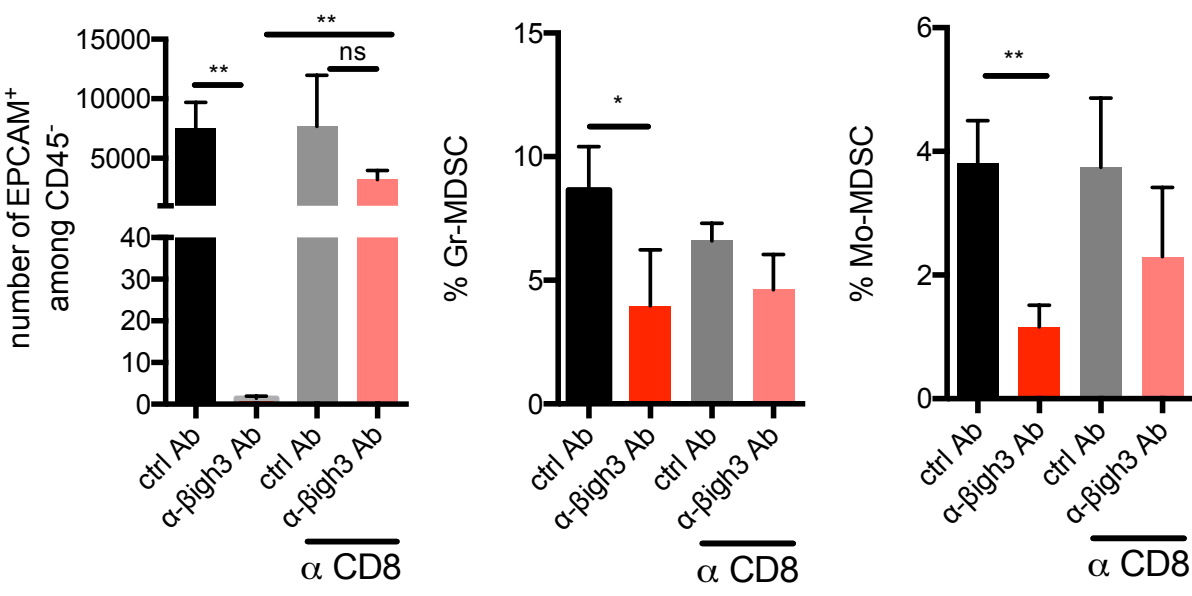
**C**



**D**

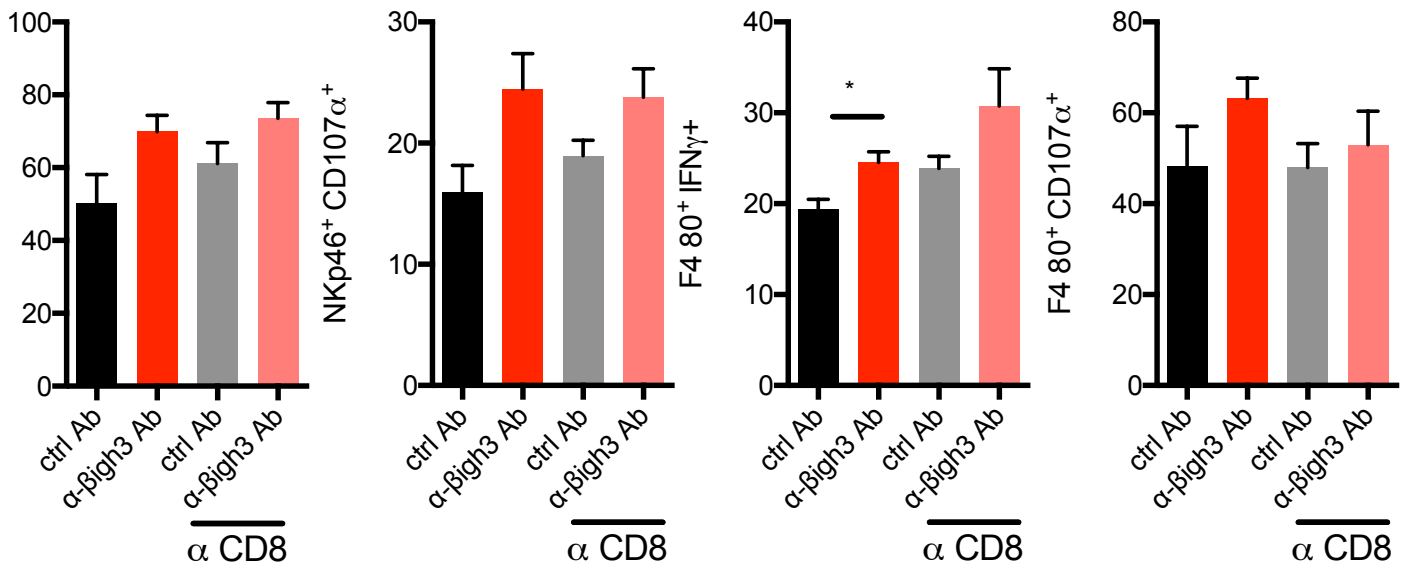


**E**

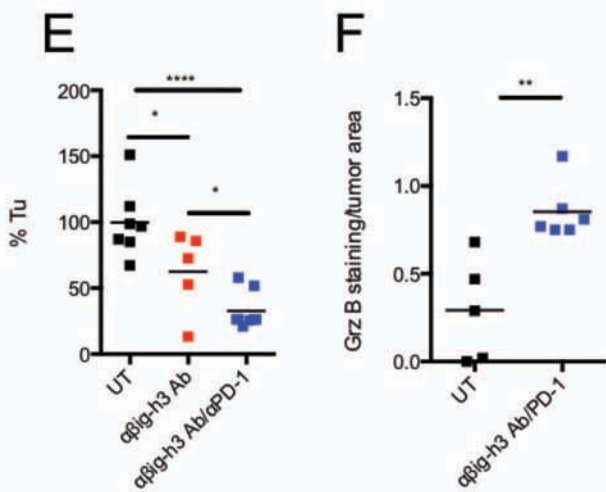
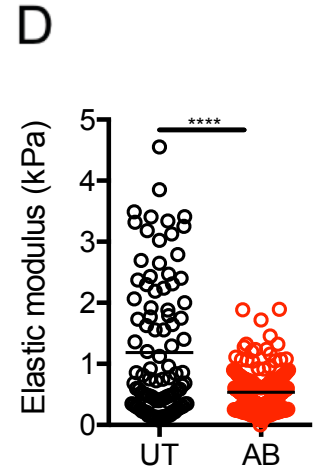
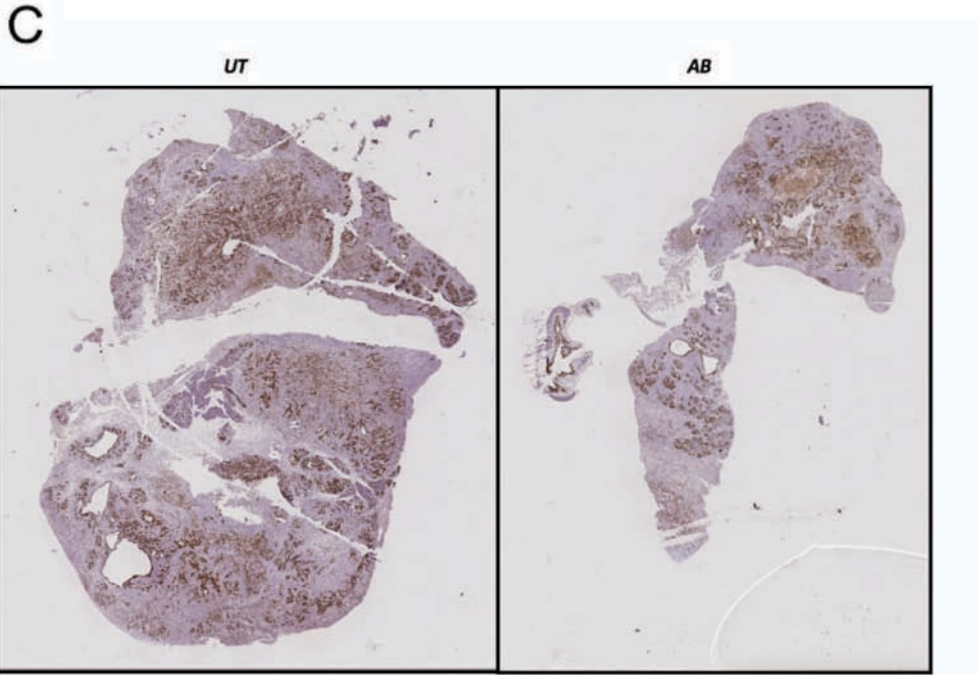
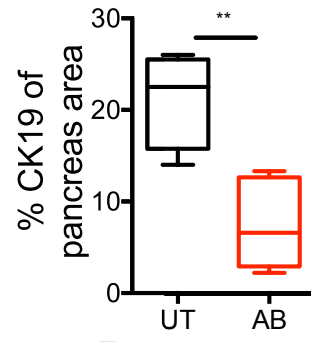
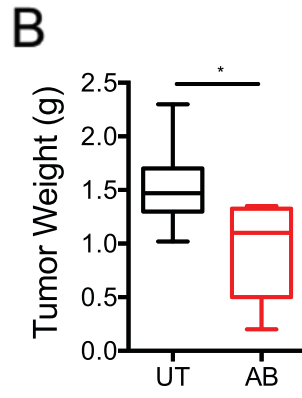
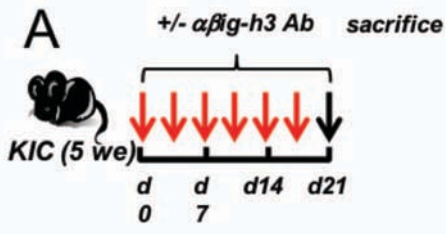


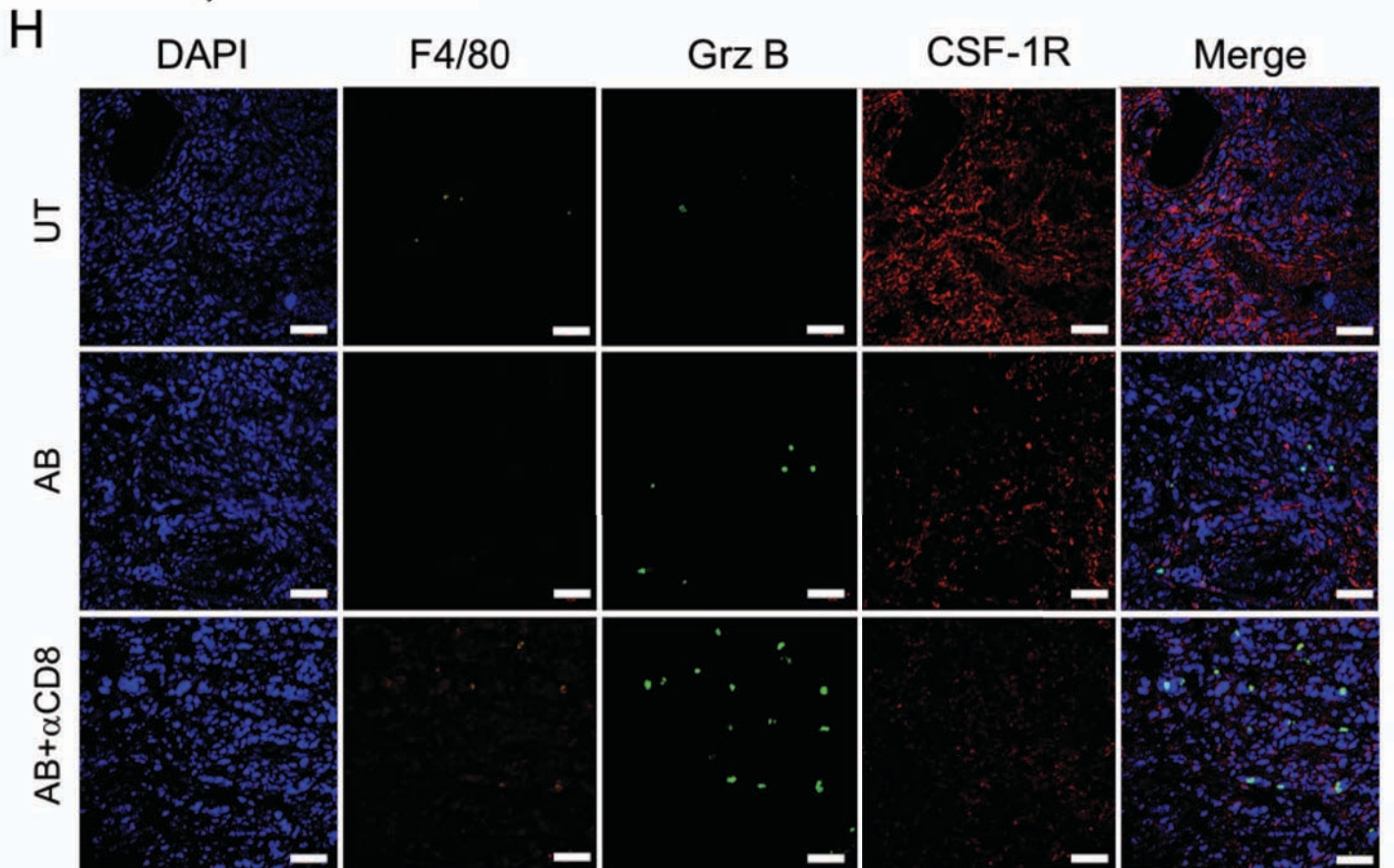
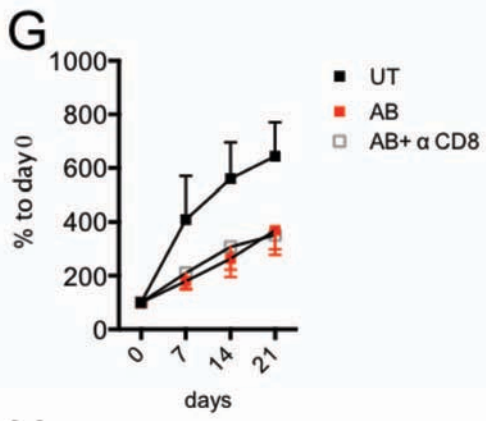


F



**Supplementary Figure 6.** FACS analysis in KC implantation in C57Bl6 mice (percentages and numbers/g tumor) of the following immune cell populations: (A) CD45<sup>+</sup> T cells, (B) CD8<sup>+</sup> T cells, (C) CD4<sup>+</sup> T cells and (D) F4/80<sup>+</sup> macrophages in C57Bl6 mice that were subcutaneously injected with KC cells that were treated with ctrl or anti-βig-h3 antibodies and then further depleted (or not) via an intravenous injection with anti-CD8 antibodies. \* $P < 0.05$ . FACS analysis in KIC implantation (percentages and numbers/g tumor) of the following populations: (E) EPCAM, Gr-MDSC, Mo-MDSC (F) NK cells, F4/80<sup>+</sup> macrophages in C57Bl6 mice that were subcutaneously injected with KIC cells that were treated with ctrl or anti-βig-h3 antibodies and then further depleted (or not) via an intravenous injection with anti-CD8 antibodies. \* $P < 0.05$ . \*\*  $P < 0.01$ .





**Supplementary Figure 7.** The impact of inducing the *in vivo* depletion of  $\beta$ ig-h3 in KIC mice. (A) Experimental protocol used to induce antibody depletion. (B) Tumoral weights were quantified at the end of the experiment. (C) Representative scan of immunohistochemistry on whole sectioned pancreas (CK19 staining). (D) Elastic Modulus quantification by AFM coupled with IF (based on CK19 and aSMA staining) in UT and AB treated KIC mice (3 independent mice per group, 100 force curves were measured per interest zone). (E) Impact of the combination anti- $\beta$ ig-h3 and anti-PD-1 Abs. The experiment was performed using 5-6 mice per group. (F) Quantification of the GrzB staining per tumoral area (on whole scan section). (G) Impact of the combination anti- $\beta$ ig-h3 and anti-CD8 Abs in KPC mice. Tumoral volume was quantified using ultrasound (Vevo2100®) in Ab-treated animals and represented in % to day 0. (H) Representative immunofluorescence stainings for F4/ 80, GrzB, CSF-R1 and DAPI in UT, AB and AB+ $\alpha$ CD8-treated mice pancreas sections. Scale bar 50  $\mu$ m \* $P < 0.05$ , \*\*  $P < 0.01$ , \*\*\*\*  $P < 0.0001$ .

384 SNP Panel Batch MB-170925KB

CR GEMS France Order 2017007016:  
pk447 Cells (SLog10) in 10% DMSO Comparison to B6J

Percent Match to Reference Allelic Profiles of Standard Inbred Strains

LTM # - Sample ID	B6J	B6N	NOD.LJ	C57BL/6J	FVB	BALB/c	BALB/cByJ	BALB/cJ	DBA/2J
001-pk447	94.8%	93.8%	46.0%	40.0%	39.6%	39.1%	39.1%	39.1%	35.1%
	94.8%	93.8%	46.0%	40.0%	39.6%	39.1%	39.1%	39.1%	35.1%

**Supplementary Table 1. 384 SNP Panel Batch MB-170925KB (Charles Rivers) was performed by to determine the C57B6J backcross phenotype.**